Biochemistry and Biophysics Reports 10 (2017) 132–136

Contents lists available at ScienceDirect

Biochemistry and Biophysics Reports

journal homepage: www.elsevier.com/locate/bbrep

Characterization of lipid rafts in human platelets using nuclear magnetic resonance: A pilot study

Joshua F. Ceñido[a], Boris Itin[b], Ruth E. Stark[c], Yung-yu Huang[a,d], Maria A. Oquendo[a,d], J. John Mann[a,d,e], M. Elizabeth Sublette[a,d,*]

[a] Department of Psychiatry, Columbia University, 1051 Riverside Drive, New York, NY 10032, USA
[b] New York Structural Biology Center, 89 Convent Avenue, New York, NY 10040, USA
[c] Department of Chemistry and Biochemistry, The City College of New York, Marshak Science Building MR-1024, CCNY, 160 Convent Avenue, New York, NY 10031, USA
[d] Division of Molecular Imaging and Neuropathology, New York State Psychiatric Institute, 1051 Riverside Drive, New York, NY 10032, USA
[e] Department of Radiology, Columbia University, 1051 Riverside Drive, New York, NY 10032, USA

ARTICLE INFO

Keywords:
NMR
Platelets
Rafts
Lipid microdomains

ABSTRACT

Lipid microdomains ('lipid rafts') are plasma membrane subregions, enriched in cholesterol and glycosphingolipids, which participate dynamically in cell signaling and molecular trafficking operations. One strategy for the study of the physicochemical properties of lipid rafts in model membrane systems has been the use of nuclear magnetic resonance (NMR), but until now this spectroscopic method has not been considered a clinically relevant tool. We performed a proof-of-concept study to test the feasibility of using NMR to study lipid rafts in human tissues. Platelets were selected as a cost-effective and minimally invasive model system in which lipid rafts have previously been studied using other approaches. Platelets were isolated from plasma of medication-free adult research participants ($n=13$) and lysed with homogenization and sonication. Lipid-enriched fractions were obtained using a discontinuous sucrose gradient. Association of lipid fractions with GM1 ganglioside was tested using HRP-conjugated cholera toxin B subunit dot blot assays. ^{1}H high resolution magic-angle spinning nuclear magnetic resonance (HRMAS NMR) spectra obtained with single-pulse Bloch decay experiments yielded spectral linewidths and intensities as a function of temperature. Rates of lipid lateral diffusion that reported on raft size were measured with a two-dimensional stimulated echo longitudinal encode-decode NMR experiment. We found that lipid fractions at 10–35% sucrose density associated with GM1 ganglioside, a marker for lipid rafts. NMR spectra of the membrane phospholipids featured a prominent 'centerband' peak associated with the hydrocarbon chain methylene resonance at 1.3 ppm; the linewidth (full width at half-maximum intensity) of this 'centerband' peak, together with the ratio of intensities between the centerband and 'spinning sideband' peaks, agreed well with values reported previously for lipid rafts in model membranes. Decreasing temperature produced decreases in the 1.3 ppm peak intensity and a discontinuity at ~18 °C, for which the simplest explanation is a phase transition from L_d to L_o phases indicative of raft formation. Rates of lateral diffusion of the acyl chain lipid signal at 1.3 ppm, a quantitative measure of microdomain size, were consistent with lipid molecules organized in rafts. These results show that HRMAS NMR can characterize lipid microdomains in human platelets, a methodological advance that could be extended to other tissues in which membrane biochemistry may have physiological and pathophysiological relevance.

1. Introduction

Lipidomics has wide implications for human health. Among the most fundamental roles for lipids is their participation in cell membranes, where they serve not only structural but also dynamic functions. Current understanding of cell membrane organization postulates the existence of lipid microdomains, or rafts, comprised principally of cholesterol and sphingolipids, which self-segregate from the surrounding phospholipid bilayer [1] due to sterically aversive forces [2]. The largely dietarily-determined lipid balance can affect the physicochemical properties of the membrane microdomains, with downstream effects on cell-cell signaling, molecular trafficking, and regulation of transmembrane proteins, including a variety of transporters and G-protein coupled receptors [3]. Among technologies used to study the composition of lipid rafts, ^{1}H detected high-resolution magic-angle spinning nuclear magnetic resonance (HRMAS NMR) utilizes the

* Corresponding author at: Division of Molecular Imaging and Neuropathology, New York State Psychiatric Institute, Unit 42, 1051 Riverside Drive, New York, NY 10032, USA.
E-mail address: sublett@nyspi.columbia.edu (M. Elizabeth Sublette).

http://dx.doi.org/10.1016/j.bbrep.2017.03.005
Received 22 December 2016; Received in revised form 28 February 2017; Accepted 15 March 2017
Available online 20 March 2017

natural proton signals from lipids to provide very good resolution of chemically shifted resonances through rapid spinning of samples at the "magic angle" (54.7°) with respect to the main magnetic field. NMR has been used to characterize lipid rafts in model membrane systems [4–9,11–14], in cell culture [15–17], and in the influenza viral envelope [18]. However, NMR has not been utilized in clinical studies of human cell membranes. Therefore we proceeded to test the feasibility of using HRMAS NMR to characterize lipid rafts in human platelets, in which lipid rafts have been successfully studied using other methods [19–22]. The NMR approach allows for physicochemical characterization of lipid rafts at the molecular level. Potential applications include studies of the effects of dietary intake of lipids (e.g., polyunsaturated fatty acids and cholesterol) and antihyperlipidemic medications on cell membrane functioning in healthy individuals and in pathological states.

2. Materials and methods

2.1. Sample

Platelets were isolated from plasma of medication-free adult research participants ($n=13$) with major depressive disorder who were otherwise medically healthy, and who had enrolled in mood disorders protocols at the New York State Psychiatric Institute and gave informed consent to the collection of blood samples for biochemical studies.

2.2. Purification of platelet lipid domains

Platelets were extracted from blood samples as previously described according to methods optimized by our research team [23]. Briefly, the blood was collected in EDTA vacutainer tubes and centrifuged at low speed to obtain the platelet-rich-plasma, which was then further centrifuged (12,000 × *g*, 4 °C, 4 min). The resulting pellets were resuspended in 5 mL of ice-cold phosphate-buffered saline (PBS, pH 7.4) and again pelleted and stored at −80 °C until used. For the next (homogenization) step, the platelet pellets were resuspended and washed twice in ice-cold PBS and suspended in 2 mL of 500 mM Na_2CO_3 solution, pH 11.0.

To avoid artifacts associated with detergent extraction [24,25], lipid rafts were isolated from extracted platelets using non-detergent methods: cells were lysed using a Polytron Homogenizer (Brinkmann, Lucerne, Switzerland; three 10-s bursts at setting 3) and then subjected to sonication with an XL-2000 Ultrasonic Cell Disruptor (Microson, Newtown, CT, USA; three 20-s bursts at setting 5). The homogenate was then adjusted to 45% sucrose by adding 2 mL of 90% sucrose prepared in 25 mM MES-buffered saline (MBS; 25 mM 2-(*N*-morpholino)ethanesulfonic acid, pH 6.5, 0.15 M NaCl). The fraction enriched in lipids was isolated by a 5–35% discontinuous sucrose gradient [5%, 15%, 25%, 35%], followed by ultracentrifugation (100,000 × *g* for 20 h at 4 °C) with flotation (adapted from [26]). Fractions containing lipids exhibited visible opalescence after ultracentrifugation (Fig. 1A). The interface was removed, diluted with 2X MBS buffer, and centrifuged (10,000 rpm for 20 min); the pellets were saved and stored at −20 °C for subsequent lipid extraction. The presence of GM1 gangliosides in the lipid fraction was assessed with GM1-specific horseradish peroxidase (HRP)-conjugated cholera toxin B subunit dot blot assays [27] using chemiluminescence (Fig. 1B). The quantity of proteins in lipid and non-lipid fractions was determined by Bicinchoninic (BCA) Protein Assay (Thermo Fisher Scientific; Rockford, IL, USA) [28] and spectrophotometry (Fig. 1C). The Folch method [29] was used to extract the lipids from the sucrose solution into an 8:4:3 chloroform-methanol-water mixture. Lipid samples were lyophilized and stored at −80 °C.

2.3. Lipid ^{1}H HRMAS NMR spectra

To prepare samples for NMR, the frozen lyophilized lipids were

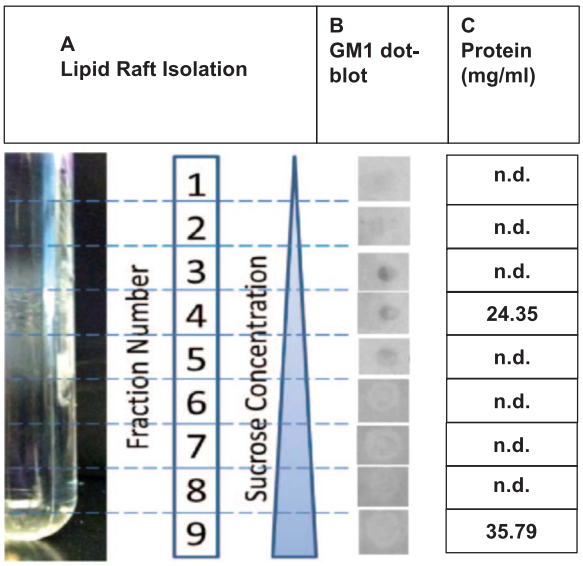

Fig. 1. Purification and validation of lipid rafts from human platelets. **A.** Visible opalescent lipid band with respect to the sucrose fractionation. **B.** GM1-specific HRP-conjugated cholera toxin B subunit dot blot assays. **C.** BCA assay differentiates between lipid-associated (fraction 4) and lipid non-associated (fraction 9) proteins; 'n.d.' indicates no protein detected.

reconstituted in deuterated water (D_2O). Five washes in D_2O were each performed by adding 300 μL of deuterated water to each sample in a microcentrifuge tube, spinning the samples at 10,000 rpm for 15 min, and decanting the clear layer using a pipette. Between each wash, samples were frozen via direct contact of the outside of the microcentrifuge tube with dry ice and thawed at room temperature followed by gentle vortexing. These freeze-thaw cycles were performed in order to facilitate H/D exchange between the solvent and membrane fragments. Samples thus prepared for HRMAS NMR were slightly viscous and visibly, uniformly opaque suspensions of multibilayers.

Butylated hydroxytoluene (BHT) was added to all samples to prevent oxidation of the unsaturated lipid acyl chains. Water-soluble 4,4-dimethyl-4-silapentane-1-sulfonic acid (DSS) was added to all samples at a ratio of 100:1 lipid:DSS by weight as a chemical shift calibration standard for NMR spectroscopy.

NMR data were acquired at the New York Structural Biology Center on a 4-channel Bruker Avance I widebore spectrometer equipped with a 4 mm HRMAS HCND probe and ZrO_2 rotors (Bruker Biospin, Karlsruhe, Germany), operating at a ^{1}H resonance frequency of 750 MHz and using a spectral width of 15 kHz. Samples were spun at an angle of 54.7° to the magnetic field direction (the 'magic angle') at spinning frequencies of 4–5 kHz to obtain well-resolved spectra. ^{1}H spectra were acquired with a single-pulse Bloch decay experiment [30] using an 8 μs 90° pulse. We acquired 128 scans with a recycle delay of 2 s between data acquisitions, thus requiring ~4 min to obtain each spectrum. The signal-to-noise ratio for the main lipid resonance was 50:1, allowing for reliable estimates of peak intensity and linewidth at half height. A presaturation water suppression technique was used to suppress the signal from residual ^{1}H nuclei in the D_2O solvent. Experiments were executed with and without a pre-acquisition echo sequence to test for the presence of broad signals [31]. Measurement temperatures were varied from −10 °C to 35 °C and calibrated with a methanol standard [32]. Sideband / centerband intensity ratios and linewidth differences of the principal lipid resonance at ~1.3 ppm were monitored *vs.* temperature, and these ratios were used to validate the presence of rafts in the L_o phase [13].

Rates of lipid lateral diffusion (signal intensity decay as a function of time) were measured in a two-dimensional stimulated echo longitudinal encode-decode experiment conducted with presaturation and bipolar gradients [33] (256 scans, gradient length 8 μs, recycle delay

2 s, gradient strengths of 2–96% in 32 steps (1 G/cm–48 G/cm), 1500 μs delay based on the length of the gradient pulse, diffusion time 100 ms).

3. Results

3.1. Purification of lipid microdomains

On sucrose gradient fractionation, a distinct opalescent band was visualized between 5% and 35% sucrose density, in fractions 3–5 (Fig. 1A), and the presence of lipid rafts was supported by GM1 ganglioside-positive dot blots in the same fractions (Fig. 1B). Chemiluminescence results (Fig. 1B) revealed that lipid fractions were positive for the presence of GM1 gangliosides, which have been associated with lipid raft domains [34]. The BCA assay was consistent with the presence of raft-associated and non-raft-associated proteins, in fractions 4 and 9, respectively (Fig. 1C).

3.2. Spectroscopic properties of purified platelet lipid fractions

As expected, the most prominent feature in the membrane phospholipid spectrum (Fig. 2) was the hydrocarbon chain 'bulk' methylene resonance at ~1.3 ppm. No broad spectral contributions were evident in data obtained without the pre-acquisition spin echo sequence, arguing against the presence of residual membrane-associated proteins or lipids in the S_o phase. Across the 4 platelet-derived lipid multibilayer samples, we observed linewidth values (full width at half-maximum intensity) for the 'centerband' methylene peak at 1.3 ppm ranging from 55 to 82 Hz at 6.5 °C, with corresponding sideband:centerband ratios amounting to 2.5–5.3%. Compared with small-molecule standards such as DSS, the centerband peak thus exhibits a clearly broadened resonance. Nonetheless, these relatively modest centerband linewidths and sideband proportions, together with the similarity in magnitude of the linewidths for the $(CH_2)_n$ centerband and sideband (shown in Fig. 2), are more characteristic of the liquid-ordered (L_o) phase identified with lipid rafts in equilibrium with a liquid-disordered (L_d) phase [6] than with a significant S_o component. Our findings are also consistent with reports of model membrane systems in which raft formation accompanied by enhanced membrane order has been associated with greater proportions of cholesterol with respect to phospholipid, producing a modestly broadened centerband peak and minor redistribution of the signal intensity from centerband to sidebands [4].

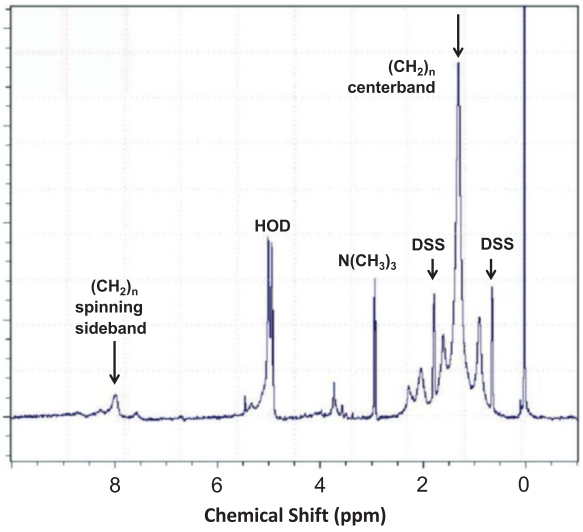

Fig. 2. Representative platelet lipid NMR spectra. From this experiment, acquired at 6.5 °C, two contributions to the lipid chain methylene resonance $(CH_2)_n$ are visible: centerband, 1.3 ppm (top arrow) and one spinning sideband, 8 ppm (left arrow) are shown. The internal chemical shift calibration standard, 4,4-dimethyl-4-silapentane-1-sulfonic acid (DSS) has two peaks (small arrows). HOD denotes H_2O in equilibrium with D_2O.

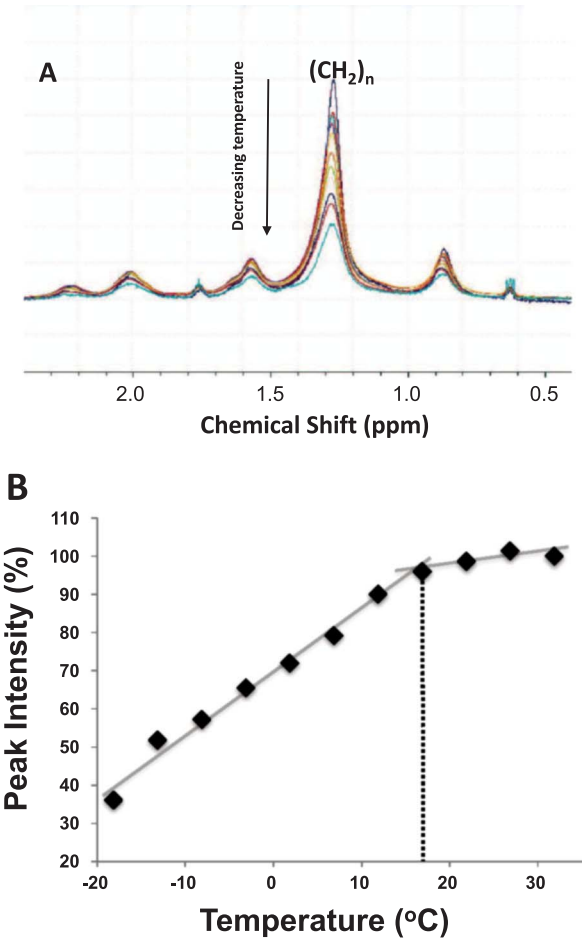

Fig. 3. Temperature dependence of peak intensity. A. Phospholipid chain methylene (1.2–1.4 ppm) spectral region for a series of ^{1}H HRMAS NMR spectra of platelet lipids acquired in a single sample at temperatures between −20 °C and 32 °C. B. Using data from A, $(CH_2)_n$ peak signal intensities at 1.3 ppm, as a percentage of the total intensity across the spectrum, are plotted as a function of temperature. A discontinuity is apparent at higher temperatures; extrapolation of the two straight-line portions yields an intersection point from which the apparent L_d to L_o phase transition temperature is estimated to be ~18 °C.

3.3. Phase transitions and raft formation demonstrated through ^{1}H NMR spectra at varying temperatures

A temperature series (Fig. 3) provides information about the phase transition between the L_d and L_o phases of our lipid-enriched platelet preparation. Decreasing height of the 1.3-ppm peak in response to decreasing temperature (Fig. 3A), which is accompanied by an increase in peak linewidth, is most simply explained by an increased predominance of L_o relative to L_d phase of the membranes [5]. In a more quantitative presentation of the data (Fig. 3B), the intensity of the 1.3-ppm peak is illustrated as a function of temperature; a discontinuity is apparent at higher temperatures, from which we estimate an L_d-to-L_o transition temperature of approximately 18 °C.

3.4. Diffusion as a measure of average domain size

The dependence of peak intensity on gradient strength is a measure of the translational diffusion constant. Diffusion is spatially restricted if the average distance that lipids move during the diffusion time is constant for a sufficiently long period. We extracted an order-of-magnitude diffusion constant of 1.4×10^{-11} m^2/s, a measure of average

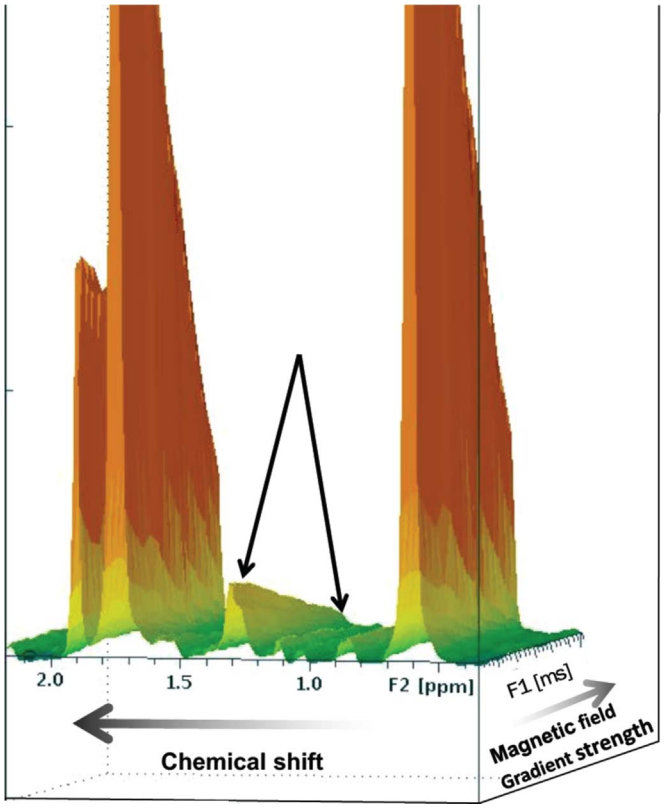

Fig. 4. Representative lipid diffusion study. This 3-D graph illustrates the methylene resonance at 1.3 ppm as a function of gradient strength. Arrows indicate decay of the lipid raft signal, which occurs approximately 3 times more slowly with gradient strength than the 4,4-dimethyl-4-silapentane-1-sulfonic acid (DSS) standard (large twin peaks flanking the methylene signal).

domain size that is in reasonable agreement with the 0.8×10^{-11} value reported previously for a model phospholipid mixture [4]. As expected, the acyl chain lipid signal at 1.3 ppm decayed more slowly with gradient strength than the reference DSS signals (Fig. 4). The membrane microdomain size indicated by the approximately three-fold lower rates of lateral diffusion we observed in comparison to the freely mobile water-soluble DSS standard is consistent with the scale estimated for lipid rafts in phospholipid model membrane mixtures [4].

4. Discussion

In platelet-derived lipid rafts, we obtain reproducible, well-resolved lipid HRMAS ^{1}H NMR spectra with minimal artifacts. Our observed linewidths, intensity ratios, and preferential broadening of sidebands agree well with values reported for lipid rafts in 30 mol% cholesterol mixtures with a single phospholipid such as 1-stearoyl-2-oleoylphosphatidylcholine [13]. We have also successfully measured lateral lipid diffusion, and we consider this estimate to be compatible with that previously reported for phospholipid mixtures in a model membrane preparation [4], given the different compositions of the respective lipid mixtures and our observation of biexponential signal decays. Our phase transition results, derived from a temperature series, can be compared with those of Veatch et al. [5], who studied a mixture of 30% cholesterol and 70% phosphatidylcholine (PC) phospholipids (dioleoylphosphatidylcholine [DOPC] + dipalmitoylphosphatidylcholine [DPPC]). Our clinical samples are expected to approximate this distribution, since human platelets are about 20% cholesterol and 70% phospholipid. The largest phospholipid fraction, ~35%, is PC, although phosphatidylinositol (~10%), phosphatidylserine (~12%), phosphatidylethanolamine (~22%) and sphingomyelin (~15%) are also present [35]. The shape of our phase transition curve (Fig. 3) resembles that of Veatch et al. [5], except the platelet membrane data are shifted to the left. The 30:70 cholesterol:PC phospholipids model membranes exhibit a L_o-to-L_d transition temperature of ~32 °C for the binary lipid mixture [5], consistent with the presence of high-melting DPPC, in contrast to an apparent L_o-to-L_d transition temperature of ~18 °C for our more complex mixture that includes phospholipid species with unsaturated acyl chains. By comparison, Fourier transform infrared spectroscopy (FT-IR) methods show phase transitions at ~15 and ~30 °C for intact platelets prepared without lipid enrichment [36].

We acknowledge that the demonstration of phase transition is not proof that functional rafts exist in the extracted fractions. In the following section we discuss combining NMR studies with biological assays to verify the presence of rafts by assessing various functional characteristics.

4.1. Potential of NMR as a clinical tool to study lipid rafts in biological membranes

Because of their renewability, platelets can provide a cost-effective and minimally invasive *ex vivo* method for studying the functions of lipid rafts in humans. Standardized methods for obtaining a detailed platelet lipid raft profile could provide a platform for understanding whether lipid raft changes mediate effects on clinical symptoms. Such methods of valuation may eventually be useful for evaluating the risk of chronic conditions already associated with lipid rafts, including Parkinson's disease [37], dementia [38], atherosclerosis [39,40], rheumatoid arthritis [41], and depression [42,43].

To approach this goal, lipid raft functional roles in cell signaling [44] and protein trafficking [45] could be studied using NMR measurement of lipid raft physicochemical properties accompanied by dynamic functional studies after perturbation or enhancement of lipid raft characteristics. For instance, lipid raft disruption by cholesterol depletion alters mobility of the serotonin transporter [46], decreases transport activity, and reduces transporter affinity for serotonin [47,48]. As another example, polyunsaturated fatty acids (PUFAs) have direct effects on the physicochemical properties of plasma membrane lipid subdomains in model membrane systems [2,7–9,11,12], and incorporation of polyunsaturated fatty acids into lipid rafts increases antibody binding to major histocompatibility complex (MHC) class I membrane proteins on certain cell types [49]. These structure-function studies have all been carried out in cell culture [46,48–50], heterologous expression systems [47] or animal models [47,50]. Our NMR technique, however, is designed to be used in studies of human platelets or other cell types. In combination with functional assays, NMR could thus be used to prospectively assess effects of dietary PUFA supplementation or cholesterol-lowering medications on activity of membrane proteins and how changes in activity relate to changes in raft structural properties.

4.2. Limitations

Potential limitations include artifacts induced by the sucrose gradient and mechanical disruption of membranes, and lack of information about the ganglioside and protein components of the system. We note that NMR spectra were monitored over a limited range of temperatures in this preliminary feasibility study. Additional studies encompassing a greater range of temperatures would be required in order to verify whether other discontinuities also occur.

5. Conclusions

Our findings introduce a novel translational application for a powerful basic science tool. NMR quantification of platelet lipid rafts can enhance other high-resolution and quantitative approaches [51,52] to the study of structural and functional characteristics of lipid microdomains. This new translational approach could have clinical utility for understanding physiology and pathophysiology at the

molecular level.

Funding

This work was supported by NIMH, MH079033 (PI: Sublette), 5P50MH062185-10, 5R01MH040695-22 (PI: Mann), 4P50MH090964-04 (PI: Oquendo), and by the National Institute on Minority Health and Health Disparities, 5G12 MD007603-30. R.E.S. is a member of the New York Structural Biology Center (NYSBC). The data collected at NYSBC was made possible by a grant from the New York State Office of Science, Technology, and Academic Research.

References

[1] K. Simons, E. Ikonen, Functional rafts in cell membranes, Nature 387 (6633) (1997) 569–572.
[2] S.R. Wassall, et al., Order from disorder, corralling cholesterol with chaotic lipids. The role of polyunsaturated lipids in membrane raft formation, Chem. Phys. Lipids 132 (1) (2004) 79–88.
[3] J.A. Allen, R.A. Halverson-Tamboli, M.M. Rasenick, Lipid raft microdomains and neurotransmitter signalling, Nat. Rev. Neurosci. 8 (2) (2007) 128–140.
[4] I.V. Polozov, K. Gawrisch, NMR detection of lipid domains, in: T.J. McIntosh (Ed.), Lipid Rafts, Himana Press, Totowa, 2007, pp. 107–126.
[5] S.L. Veatch, et al., Liquid domains in vesicles investigated by NMR and fluorescence microscopy, Biophys. J. 86 (5) (2004) 2910–2922.
[6] I.V. Polozov, K. Gawrisch, NMR detection of lipid domains, Methods Mol. Biol. 398 (2007) 107–126.
[7] S.P. Soni, et al., Docosahexaenoic acid enhances segregation of lipids between raft and non-raft domains: 2H-NMR study, Biophys. J. 95 (1) (2008) 203–214.
[8] N.V. Eldho, et al., Polyunsaturated docosahexaenoic vs docosapentaenoic acid-differences in lipid matrix properties from the loss of one double bond, J. Am. Chem. Soc. 125 (21) (2003) 6409–6421.
[9] S.R. Shaikh, et al., Oleic and docosahexaenoic acid differentially phase separate from lipid raft molecules: a comparative NMR, DSC, AFM, and detergent extraction study, Biophys. J. 87 (3) (2004) 1752–1766.
[11] M. Mihailescu, et al., Structure and dynamics of cholesterol-containing polyunsaturated lipid membranes studied by neutron diffraction and NMR, J. Membr. Biol. 239 (1–2) (2011) 63–71.
[12] J.A. Williams, et al., Docosahexaenoic and eicosapentaenoic acids segregate differently between raft and nonraft domains, Biophys. J. 103 (2) (2012) 228–237.
[13] I.V. Polozov, K. Gawrisch, Characterization of the liquid-ordered state by proton MAS NMR, Biophys. J. 90 (6) (2006) 2051–2061.
[14] G.P. Holland, S.K. McIntyre, T.M. Alam, Distinguishing individual lipid headgroup mobility and phase transitions in raft-forming lipid mixtures with 31P MAS NMR, Biophys. J. 90 (11) (2006) 4248–4260.
[15] L.C. Wright, et al., Detergent-resistant membrane fractions contribute to the total 1H NMR-visible lipid signal in cells, Eur. J. Biochem. 270 (9) (2003) 2091–2100.
[16] M. Harris, et al., Membrane disordering by eicosapentaenoic acid in B lymphomas is reduced by elongation to docosapentaenoic acid as revealed with solid-state nuclear magnetic resonance spectroscopy of model membranes, J. Nutr. 146 (7) (2016) 1283–1289.
[17] A. Ferretti, et al., High-resolution proton NMR measures mobile lipids associated with Triton-resistant membrane domains in haematopoietic K562 cells lacking or expressing caveolin-1, Eur. Biophys. J. 32 (2) (2003) 83–95.
[18] I.V. Polozov, et al., Progressive ordering with decreasing temperature of the phospholipids of influenza virus, Nat. Chem. Biol. 4 (4) (2008) 248–255.
[19] N. Dionisio, et al., Lipid rafts are essential for the regulation of SOCE by plasma membrane resident STIM1 in human platelets, Biochim. Biophys. Acta 1813 (3) (2011) 431–437.
[20] S.J. Israels, E.M. McMillan-Ward, Platelet tetraspanin complexes and their association with lipid rafts, Thromb. Haemost. 98 (5) (2007) 1081–1087.
[21] V. Rabani, et al., Comparative lipidomics and proteomics analysis of platelet lipid rafts using different detergents, Platelets 27 (7) (2016) 634–641.
[22] S. Reineri, et al., Membrane lipid rafts coordinate estrogen-dependent signaling in human platelets, Biochim. Biophys. Acta 1773 (2) (2007) 273–278.
[23] V.D. Khait, Y.Y. Huang, J.J. Mann, Methodological considerations for the human platelet 5-HT2A receptor binding kinetic assay, Life Sci. 65 (24) (1999) 2615–2622.
[24] E.B. Babiychuk, A. Draeger, Biochemical characterization of detergent-resistant membranes: a systematic approach, Biochem. J. 397 (3) (2006) 407–416.
[25] D. Lichtenberg, F.M. Goni, H. Heerklotz, Detergent-resistant membranes should not be identified with membrane rafts, Trends Biochem. Sci. 30 (8) (2005) 430–436.
[26] P. Maurice, et al., The platelet receptor for type III collagen (TIIICBP) is present in platelet membrane lipid microdomains (rafts), Histochem. Cell Biol. 125 (4) (2006) 407–417.
[27] J. Holmgren, et al., Interaction of cholera toxin and membrane GM1 ganglioside of small intestine, Proc. Natl. Acad. Sci. USA 72 (7) (1975) 2520–2524.
[28] P.K. Smith, et al., Measurement of protein using bicinchoninic acid, Anal. Biochem. 150 (1) (1985) 76–85.
[29] J. Folch, M. Lees, G.H. Sloane Stanley, A simple method for the isolation and purification of total lipids from animal tissues, J. Biol. Chem. 226 (1) (1957) 497–509.
[30] F. Bloch, Nuclear Induction, Phys. Rev. 70 (1946) 460.
[31] H.Y. Carr, E.M. Purcell, Effects of diffusion on free precession in nuclear magnetic resonance experiments, Phys. Rev. 94 (3) (1954) 630–638.
[32] C. Ammann, P. Meier, A.E. Merbach, A simple multinuclear NMR thermometer, J. Magn. Reson. 46 (1982) 319–321.
[33] D.H. Wu, A. Chen, C.S. Johnson, Flow imaging by means of 1d pulsed-field-gradient NMR with application to electroosmotic flow, J. Magn. Reson. Ser. A 115 (1) (1995) 123–126.
[34] R.W. Ledeen, G. Wu, The multi-tasked life of GM1 ganglioside, a true factotum of nature, Trends Biochem. Sci. 40 (7) (2015) 407–418.
[35] R.M. Dougherty, et al., Lipid and phospholipid fatty acid composition of plasma, red blood cells, and platelets and how they are affected by dietary lipids: a study of normal subjects from Italy, Finland, and the USA, Am. J. Clin. Nutr. 45 (2) (1987) 443–455.
[36] K. Gousset, et al., Evidence for a physiological role for membrane rafts in human platelets, J. Cell Physiol. 190 (1) (2002) 117–128.
[37] N. Fabelo, et al., Severe alterations in lipid composition of frontal cortex lipid rafts from Parkinson's disease and incidental Parkinson's disease, Mol. Med. 17 (9–10) (2011) 1107–1118.
[38] K. Sasahara, K. Morigaki, K. Shinya, Effects of membrane interaction and aggregation of amyloid beta-peptide on lipid mobility and membrane domain structure, Phys. Chem. Chem. Phys. 15 (23) (2013) 8929–8939.
[39] S. Lemaire-Ewing, L. Lagrost, D. Neel, Lipid rafts: a signalling platform linking lipoprotein metabolism to atherogenesis, Atherosclerosis 221 (2) (2012) 303–310.
[40] B. Catalgol, N. Kartal Ozer, Lipid rafts and redox regulation of cellular signaling in cholesterol induced atherosclerosis, Curr. Cardiol. Rev. 6 (4) (2010) 309–324.
[41] E. Janas, et al., Rituxan (anti-CD20 antibody)-induced translocation of CD20 into lipid rafts is crucial for calcium influx and apoptosis, Clin. Exp. Immunol. 139 (3) (2005) 439–446.
[42] A.H. Czysz, M.M. Rasenick, G-Protein signaling, lipid rafts and the possible sites of action for the antidepressant effects of n-3 polyunsaturated fatty acids, CNS Neurol. Disord. Drug Targets 12 (4) (2013) 466–473.
[43] R.J. Donati, et al., Postmortem brain tissue of depressed suicides reveals increased Gs alpha localization in lipid raft domains where it is less likely to activate adenylyl cyclase, J. Neurosci. 28 (12) (2008) 3042–3050.
[44] D. Lingwood, K. Simons, Lipid rafts as a membrane-organizing principle, Science 327 (5961) (2010) 46–50.
[45] A.W. Cohen, et al., Role of caveolae and caveolins in health and disease, Physiol. Rev. 84 (4) (2004) 1341–1379.
[46] J.C. Chang, et al., Single molecule analysis of serotonin transporter regulation using antagonist-conjugated quantum dots reveals restricted, p38 MAPK-dependent mobilization underlying uptake activation, J. Neurosci. 32 (26) (2012) 8919–8929.
[47] F. Magnani, et al., Partitioning of the serotonin transporter into lipid microdomains modulates transport of serotonin, J. Biol. Chem. 279 (37) (2004) 38770–38778.
[48] S.M. Scanlon, D.C. Williams, P. Schloss, Membrane cholesterol modulates serotonin transporter activity, Biochemistry 40 (35) (2001) 10507–10513.
[49] S.R. Shaikh, et al., Docosahexaenoic acid modifies the clustering and size of lipid rafts and the lateral organization and surface expression of MHC class I of EL4 cells, J. Nutr. 139 (9) (2009) 1632–1639.
[50] B.D. Rockett, et al., Fish oil increases raft size and membrane order of B cells accompanied by differential effects on function, J. Lipid Res. 53 (4) (2012) 674–685.
[51] C. Klose, M.A. Surma, K. Simons, Organellar lipidomics–background and perspectives, Curr. Opin. Cell Biol. 25 (4) (2013) 406–413.
[52] H.J. Kaiser, et al., Order of lipid phases in model and plasma membranes, Proc. Natl. Acad. Sci. USA 106 (39) (2009) 16645–16650.